Handover-Aware Scheduling for Small-and Large-Scale VLC Networks

Mahmoud Wafik Eltokhey, Mohammad Ali Khalighi, Zabih Ghassemlooy, Volker Jungnickel

Handover-Aware Scheduling for Small- and Large-Scale VLC Networks

Mahmoud Wafik Eltokhey, Mohammad Ali Khalighi, Zabih Ghassemlooy, Volker Jungnickel

***Abstract*—This paper proposes handover-aware scheduling solutions for multi-cell small- and large-scale visible-light communication networks, enabling soft handover. For this, we coordinate the transmissions at the access points (APs), serving the users in different time slots based on their locations with respect to the AP coverage areas for an efficient utilization of the resources. For scenarios where coverage in large areas is needed, we additionally propose clustering solutions to decrease the handover rate. Compared with non-coordinated schemes, the proposed soft handover techniques offers improved performance in terms of user achievable throughput and link reliability.**

***Index Terms*—Visible-light communications; multi-cell networks; inter-cell interference; soft handover; scheduling.**

I. Introduction

Visible-light communication (VLC) is considered as a candidate for the sixth generation (6G) wireless networks, to resolve radio-frequency (RF) spectrum congestion, especially in indoor scenarios. The ongoing increase in the number of user devices, the multimedia quality, and the emerging applications (e.g., virtual reality), as well as the spectrum licensing costs, encourage exploring new solutions to complement RF, to keep up with the demand for the network traffic. VLC uses the existing lighting infrastructure for wireless communications. It operates in the unlicensed optical spectrum, is robust against RF electromagnetic interference, and provides inherent physical layer security in the illuminated area. As light does not penetrate through walls, the VLC network is not interfered by transmissions in adjacent rooms, hence, a more efficient and reliable resource utilization can be done, compared to RF networks [1]. In indoor areas, a multi-cell architecture can be used based on multiple light-emitting diode (LED) luminaires, each acting as an access point (AP) that handles the users within its illumination area (i.e., cell). There, users within the coverage areas of one or more APs can be classified as cell-center users (CCUs) or cell-edge users (CEUs), respectively [2]. To mitigate multi-user interference, efficient management of the resources using multiple access (MA) techniques should be used [3].

M. W. Eltokhey is with the Computer, Electrical and Mathematical Science and Engineering Division, King Abdullah University of Science and Technology, Thuwal 23955, Saudi Arabia.

M. A. Khalighi is with the Aix-Marseille University, CNRS, Centrale Marseille, Institut Fresnel, Marseille, France.

Z. Ghassemlooy is with Optical Communications Research Group, Faculty of Engineering and Environment, Northumbria University, Newcastle upon Tyne, NE1 8ST, UK.

V. Jungnickel is with Fraunhofer Heinrich-Hertz-Institute, Einsteinufer 37, 10587 Berlin, Germany.

This work was based upon work from European Union's Horizon 2020 COST Action CA19111 (NEWFOCUS).

One of the challenges associated with MA management in multi-cell VLC networks is to maintain the connectivity during transitions between cells, for which efficient handover techniques should be designed. In general, handover can be done between APs of different or the same wireless access technologies, referred to as vertical and horizontal handover, respectively [4], [5]. We consider horizontal handover here, which we refer simply to as "handover". Note that the handover solutions proposed for RF technologies, including those designed for short-range networks, are not directly applicable to VLC networks due to several factors including:

(i) the placement of the VLC APs (LED-based luminaires) in indoor scenarios mainly follows illumination (and sometimes aesthetic) considerations, in contrast to RF technologies where AP placement is engineered to maximize the communication system performance;
(ii) for the same reason, the directivity of the VLC APs is usually not controlled, in contrary to RF-based technologies where the AP antennas' beam patterns can be adjusted to optimize the performance;
(iii) there is a higher probability of large overlapping between the cell coverage areas in VLC networks due to (i) and (ii). This can result in large areas within which users suffer from high levels of inter-cell interference (ICI). On the contrary, in RF-based communication, the placement and the directivity of the antennas can be designed to minimize ICI and/or to maximize the resource reuse.

Depending on resource utilization in the employed MA technique, handover algorithms can be classified into "soft" and "hard" schemes. In the former, the user establishes data connection with the new AP before breaking the connection with the initial AP, to avoid connection disruptions. On the other hand, in hard handover, the user disconnects from the initial AP before connecting to the new one.

Handover management in VLC networks has been receiving increasing attention, due to the potentially large number of high data-rate connections in a multi-cell VLC network, as well as the impact of handover algorithm on the network performance [6]. In [7], handover was studied for the cases of overlapping and non-overlapping cells in a VLC network. Also, [8] investigated handover modelling accounting for the receiver (Rx) mobility and orientation, while [9] analyzed the performance of a multi-tier LiFi network with handover between the primary and secondary tiers. In [10], coverage areas of the APs were controlled to improve handover efficiency and user distribution in cells. Also, handover skipping was proposed in [11], which used the rate of change of received signal

power to mitigate unnecessary handovers. In [12], the use of control tone signals for managing the handover in indoor VLC systems was considered, which offered a solution for determining the AP information with the user's mobility. For vehicular VLC networks, frequency diversity-based handover solutions and low-latency handover schemes were proposed in [13] and [14], respectively, while soft handover solutions were proposed in [15]–[17], yet, without focusing on the efficiency of resource utilization. In particular, in [15], hard handover and coordinated multipoint transmission (CoMP) decisions were proposed based on received signal strength but the effect of handover delay and the efficiency of resource utilization were not investigated. Also, a soft handover scheme was proposed in [16] for multi-cell VLC networks, assuming hexagonal cells. However, this may not be realizable in practice due to the need for a unique deployment of the APs. In addition, using the considered fractional resource reuse scheme may decrease the resource utilization efficiency due to not taking into account the number of users. Lastly, in [17], soft handover was experimentally evaluated in VLC networks for the simple case of two transmitters (Txs).

In this paper, we propose efficient soft handover solutions allowing improved network sum-rate performance based on efficient resource utilization and joint transmission of adjacent APs. For this, appropriate solutions are developed for small- and large-scale deployment scenarios. For the former case, we propose scheduling the transmissions of the APs based on the strengths of the received signals, which can be represented by the locations of the Rxs with respect to the AP coverage areas. The APs transmissions are then coordinated to achieve soft-handover for mobile users while maximizing the resource utilization to improve the network sum-rate performance. This uses zones in the intersections of the APs coverage areas, where they can achieve interference-free simultaneous transmissions of users data. We will call this approach *handover-aware scheduling*. For large-scale VLC networks and potentially increased user mobility, we extend the proposed scheme to multiple cluster networks, where each cluster is composed of APs that broadcast the user signals within the coverage area of the cluster, in order to decrease the rate of handovers. There, given the larger intersection areas between the clusters, careful resource management is performed. Compared with the conventional (non-coordinated) schemes, we show that the proposed handover-aware scheduling offers improved sum-rate and connection reliability. In particular, compared to [15], [16], the novelty of our approach is to maximize the efficiency of resource utilization to improve the overall network performance while accounting for the handover delay. In addition, our proposed schemes decrease the dependence on the room architecture and can be used in practical VLC AP deployments. More specifically, the contributions of our work can be summarized as follows:

- Proposing handover-aware scheduling supporting soft handover in small-scale VLC networks while maximizing the efficiency of resource utilization;
- Extending the proposed technique to the case of multiple clusters architecture in large-scale VLC networks;
- Evaluating the performance of the proposed schemes for both of single and multiple clusters, while accounting for the effect of handover delay, and comparing the results with non-scheduling based approaches.

The remainder of the paper is organized as follows: Section II presents the system model and the main assumptions. Next, Sections III and IV describe the proposed handover-aware scheduling for small- and large-scale VLC networks, respectively. Then, Section V discusses the considered time-scheduling strategies, and Section VI presents the numerical results. Lastly, Section VII concludes the paper.

II. Main Assumptions

We consider a multi-cell VLC network, as shown in Fig. 1, in which N_t APs provide illumination and communication for N_r users, where the resource management using MA techniques is carried out in the time domain. The APs project identical Lambertian beam patterns on the floor, where in the overlapping coverage areas of the APs, users are prone to ICI. Note that, the uplink in such VLC networks could be realized using infrared links, to mitigate the interference with the downlink and also for user's convenience[1]. To manage data transmission in the whole network, we consider a centralized architecture, where a central unit classifies the users into CCUs or CEUs, takes the handover related decisions, and carries out most computation and synchronization tasks. It is similar to the centralized architecture in [19], where the luminaires can be considered as distributed units, and a fronthaul network connects all distributed units with the central unit. Note that, the CSI can be estimated at each Rx based on the transmission of some pilot symbols from the APs in the downlink, before being sent back in the uplink to the APs. Assuming the dominance of line-of-sight (LOS) transmission, the DC channel gain between the i^{th} AP (AP_i) and the j^{th} user (Rx_j) is defined as [20], [21]:

$$h_{ij} = \mathcal{R}\,\mathcal{S}\,\frac{(m+1)\,A_{\text{PD}}}{2\pi\, l_{ij}^2}\cos^m(\phi_{ij})\cos(\theta_{ij}), \tag{1}$$

where ϕ_{ij} and θ_{ij} are the angles of emission from the AP and the incidence at the Rx, respectively, and l_{ij} denotes the distance between AP_i and Rx_j. Also, $\mathcal{R}$ and A_{PD} are the PD responsivity and detection area, and $\mathcal{S}$ and m are the conversion efficiency and Lambertian order of the LED, respectively. Note, $h_{ij} = 0$ in the case θ_{ij} exceeds the field-of-view (FOV) of Rx_j.

To describe the proposed handover-aware scheduling, we consider two cases of single and multiple cluster-based VLC networks for which the architecture and the resource utilization are illustrated in Fig. 2. In the single cluster case, which is typical of small size spaces, the ensemble of APs is considered as one cluster, where they coordinate transmissions to serve the CEUs. The latter case is relevant for relatively large spaces such as large exhibition halls, industrial scenarios, etc., where managing handover becomes more critical due to potentially higher user mobility and larger number of users. Here, with

[1]Note that, carrier-sense MA with collision avoidance (CSMA/CA) could be used for handling the uplink transmission, as suggested in [18].

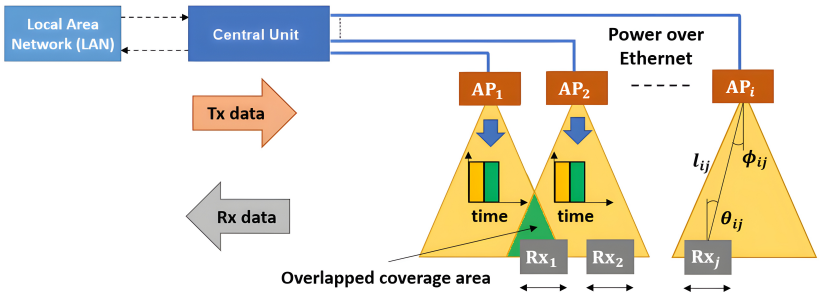

Fig. 1: Illustration of the considered VLC system, highlighting the connection of the APs to the local network via the central unit, and the management of the resources in the time domain according to the users' locations with respect to the overlapping coverage areas.

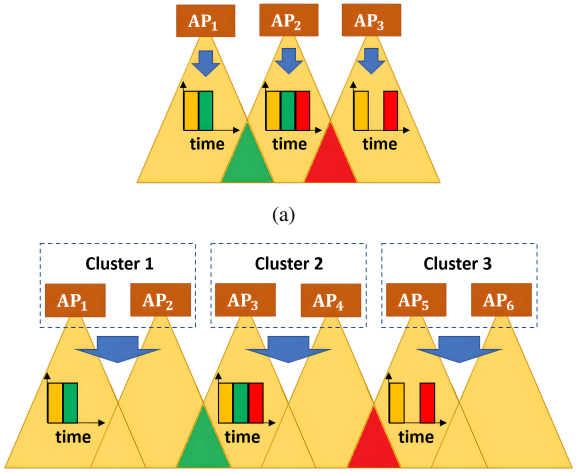

Fig. 2: Illustration of the time resource utilization with respect to the coverage areas of the: (a) single cluster, and (b) multiple cluster VLC network architecture examples, highlighting the joint transmission in the overlapped coverage areas.

TABLE I: List of main acronyms

Acronym	Definition
CCU	Cell-center user
CEU	Cell-edge user
AP_H	Host AP
AP_T	Target AP
P_H	Power received from AP_H
P_T	Power received from AP_T
C_H	Host cluster
C_T	Target cluster
C_{TR}	Transition cluster
P_{CH}	Power received from C_H
P_{CT}	Power received from C_T
P_{CTR}	Power received from C_{TR}
TTT	Time-to-trigger
HOM	Handover margin
TS	Time slot

the multiple cluster architecture, each cluster of APs broadcast signals to the users within its coverage area[2], whereas the users located at the areas of intersections are served by joint transmission of clusters. Again, a centralized network architecture is considered, where a central unit is connected to all APs. For both of single and multiple cluster cases, at the start of each transmission period, the APs broadcast packets which specify the size and the timing details of the time slots, and the user devices that are served within each time slot. Table I shows a list of the main acronyms and symbols.

III. Handover-Aware Scheduling for Single Cluster Network

In the single-cluster case, the central unit manages the transmission scheduling of each AP over a defined transmission period T using multiple time slots (TSs) in order to mitigate interference, to maximize resource utilization, and to realize handover. The handover decisions are made by the central unit, based on the received signal strength at the users devices, which allows accounting for random Rx orientations. Here, for simplicity, and in order to describe more clearly the proposed scheme, we assume that all Rxs are oriented towards the ceiling, so that the received signal strength is only represented by the Rx location. The proposed scheme is illustrated in Fig. 3 for a 4-cell VLC network, where TSs allocated to the users are set based on their locations with respect to the APs. In TS #1, all CCUs are handled simultaneously, as they are not affected by ICI. CEUs, on the other hand, are served in the next three separate TSs (#2, #3, and #4), where the users' data are broadcast by more than one AP, generating joint transmission for the CEUs, while avoiding ICI. For TSs #2 and #3, each pair of APs serves their users simultaneously, to maximize both the network resource utilization and sum-rate.

A. Conventional Handover Process

Consider first the case of conventional, i.e., non-coordinated handover process, illustrated in Fig. 4, which is, for instance, typically used in LTE cellular networks [23]. Consider a user served by an initial AP, (called here the 'Host' AP and denoted by AP_H), with the received power P_H. This user moves to the coverage area of a new AP (called the 'Target' AP and denoted by AP_T), with the corresponding received power from AP_T denoted by P_T. When P_T is larger than a pre-defined threshold P_C (defined based on the transmit power of AP, electrical to optical conversion efficiency, responsivity of the PD at the Rx, and the cell radius, etc.), the strengths of the received signals

[2]Note that, this can be done by either broadcasting the same signal or by zero-forcing pre-coding of the users signals [22] (if the number of users per cluster does not exceed the number of APs) to reduce the need to intra-cluster handovers, reducing hence the network complexity and the handover rate.

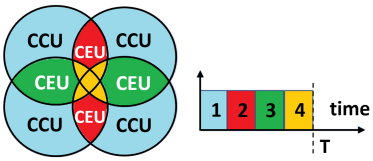

Fig. 3: Top view for AP coverage areas and the corresponding resource utilization for the proposed handover-aware scheduling. Each AP handles its CCUs (blue areas) simultaneously without experiencing ICI. In the other areas (in red, green, or yellow), each AP handles the users in the associated time slot, allowing users to benefit from spatial diversity. Note, slots durations depend on the traffic served in the different zones.

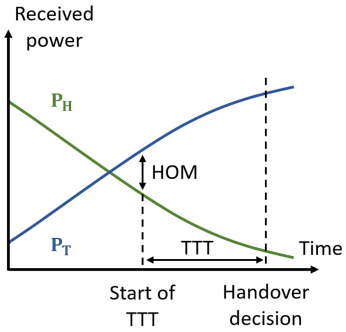

Fig. 4: Illustration of the non-coordinated handover process.

from both AP_H and AP_T are compared. Then, when P_T is larger than P_H by a so called *handover margin* (HOM) during a continuous duration of *time-to-trigger* (TTT), handover to AP_T is initiated. The time needed to effectively transfer the user to AP_T and to start receiving data from it is referred to as the *handover delay*.

In summary, consider a user firstly handled by AP_H as a CCU, before moving to the overlapping area of AP_H and AP_T. There, it starts checking if it meets the handover condition, while receiving data from AP_H. After satisfying the condition: "$P_T \geq P_H$ + HOM over TTT", handover is initiated to AP_T: The user is disconnected from AP_H, and starts receiving data from AP_T only after the handover delay, which results in link interruption in the meanwhile.

B. Proposed Coordinated Handover Approach

Consider the case of a CCU which is initially in the coverage area of AP_H, and moves to the coverage area of AP_T. When the user reaches a location at the intersection between the coverage areas of AP_T and AP_H (i.e., becomes a CEU), and where $P_T > P_C$, handover process to AP_T is initiated while keeping the connection with AP_H. Here, the user data is sent over a new CEU TS. As a result, the user remains connected to AP_H during handover delay, thus resulting in no link interruption (in contrary to the non-coordinated scheme). Here, the handover delay is the delay needed for the user to start receiving data from AP_T, so that it can be served simultaneously by AP_H and AP_T in a CEU TS. Then, in the case the user keeps moving towards AP_T and ends up as a CCU within its coverage area, the user's data is managed in a CCU TS of AP_T. As the handover of the user to AP_T already occurred in the cell-edge area, the user starts receiving the data from AP_T without additional delay.

Algorithm 1 Handover-Aware Scheduling (Single Cluster Case)

Input: P_H, P_T, P_C
Output: handover decision, TSs duration

1: **if** $P_T > P_C$ **then**
2: find TS associated with user location
3: do handover to AP_T
4: calculate new TSs duration
5: move user data to corresponding TS
6: start D_T timer
7: **while** $D_T <$ handover delay **do**
8: receive data from AP_H
9: increment D_T timer
10: receive data from AP_H and AP_T
11: reset D_T timer

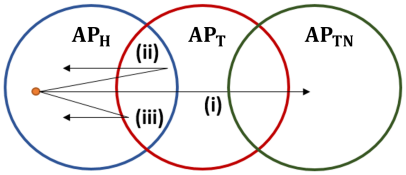

Fig. 5: Illustration for possible handover scenarios for a user (shown in orange spot), highlighting the short cell dwell time (Case (i)), and the ping-pong effect (Cases (ii) and (iii)). The blue, red, and green cells correspond to the coverage areas of AP_H, AP_T, and the new target AP (AP_{TN}), respectively.

We have provided in Algorithm 1 the pseudo-code of the proposed handover-aware scheduling to explain the operation in the transition interval where a CCU handled by AP_H moves to the intersection area of AP_H and AP_T. Here, D_T denotes the timer used for handover delay calculation. Note that, handover triggering starts once the user enters the cell edge area, where the handover delay timer starts as soon as the handover decision is made. In fact, Steps 2, 3, 4, 5, and 6 in Algorithm 1 start directly (almost in parallel) after the handover decision. For the handover of a user, once it is in the CEU area (Step 1, Algorithm 1), it is allocated a CEU time slot (Steps 2 and 5) within which AP_H will continue serving the user while AP_T will wait for the handover delay (Step 8). After the handover delay, AP_H and AP_T will transmit data simultaneously in the time slot to serve the user (Step 10). Note that, after soft handover to AP_T, the link will not be released from AP_H as long as the user lies within its coverage; this way, it will benefit from spatial diversity in increasing the received signal-to-noise ratio (SNR) while not being affected by any multi-user interference.

C. Comparison with the Conventional Approach

To compare the coordinated and conventional schemes, we consider specifically two rather critical situations:

- ✓ *Short cell dwell time*, where a user arrives for a short time in a cell before moving to a new one;
- ✓ *Ping-pong* effect, where a user moves to a new cell and then returns back to the initial cell after a short time.

To contrast the two approaches of conventional and coordinated handover, we consider three different handover-related

scenarios depending on user mobility possibilities, shown in Fig. 5. At first, the considered user is in the cell-center area of AP_H when it moves to the intersection area of AP_H and AP_T. Then, the three possible scenarios are:

- Scenario (i): The user moves to the cell-center area of AP_T, and then arrives at the intersection area between AP_T and the new target (AP_{TN}) within a short time of establishing the handover to AP_T, resulting in a short cell dwell time. At this moment:
  – For the case of non-coordinated scheme, the network has to: (1) terminate the user's link with AP_T after meeting the handover condition, i.e., "$P_{TN} \geq P_T$ + HOM over TTT", with P_{TN} denoting the received power from AP_{TN}; and (2) the user should wait for handover delay before receiving data from AP_{TN}.
  – For the case of coordinated scheme, handover is initiated to AP_{TN}, while the user receives data from AP_T; after the handover delay, it is jointly served by AP_T and AP_{TN} in a CEU TS.
- Scenario (ii): The user stays within the cell-edge area, and then moves back to AP_H (ping-pong effect).
  – For the non-coordinated scheme, if "$P_H \geq P_T$ + HOM over TTT", handover is initiated to AP_H. Then, the user's connection with AP_T is terminated and it starts receiving data from AP_H after handover delay, thus resulting in link interruption.
  – In the case of coordinated handover, there will be no change in the user's data handling; it will continue being served by both AP_H and AP_T in a CEU TS.
- Scenario (iii): The user moves back to the AP_H cell-center area with a high speed (again a ping-pong effect).
  – For the non-scheduling scheme, this may result in no coverage from AP_T prior to performing handover to AP_H. Note, additional link interruptions will occur in this case because the user has to wait before receiving data from AP_H for satisfying the handover power condition over TTT, and then, for the duration of handover delay.
  – For the coordinated scheme, the user data will be moved to a CCU TS with no link interruption, as the connection to AP_H had been already established.

In summary, compared to the conventional scheme, for the three considered scenarios, the proposed handover-aware scheduling offers higher link reliability and seamless connectivity, by benefiting from the joint transmission by the APs covering the overlapping areas between cells.

D. Network Throughput

To evaluate the network throughput, let P_e and σ_n^2 denote the transmit electrical power per AP, and the Rx noise variance, respectively. The SNR for the Rx_j is given by:

$$\mathrm{SNR}_{\mathrm{Rx}_j} = \frac{\sum_{i=1}^{N_t} h_{ij}^2 P_e}{\sigma_n^2}, \tag{2}$$

where $h_{ij} = 0$ if Rx_j is not within the coverage area of AP_i. If Rx_j is served in a TS of duration d over the transmission period T, the achievable throughput is[3]:

$$R_{\mathrm{Rx}_j} = \frac{d}{T} B \log_2\left(1 + \mathrm{SNR}_{\mathrm{Rx}_j}\right) \quad \text{(in bps)}, \tag{3}$$

where B is the link bandwidth.[4] Note that in order to avoid multi-user interference, each AP serves its users in different time slots. For CEUs, which are placed in the intersecting coverage areas of multiple APs, the transmissions of the APs are coordinated so that each CEU receives its signals from all the APs covering its location in the same time slot as illustrated in Fig. 3. This results in the summation of the signals in the numerator of (2) rather than adding the interference term in the denominator. Note, the new APs do not contribute to the numerator of (2) during the handover delay.

IV. Handover-Aware Scheduling for Multiple Cluster Network

For the case of large communication spaces, we adopt a multiple cluster architecture, as explained in Section II. Here, to manage inter-cluster handovers, we extend the idea of handover-aware scheduling presented in the previous section for the case of single cluster networks, to realize soft inter-cluster handovers. Note that, the handover decisions are made based on the received signal strength at the Rxs. For a more clear description of the proposed solution, we again assume that all Rxs are pointing upwards, so that the received signal strengths are represented by the Rxs locations.

A. AP Clustering

Figure 6 shows an illustration of the proposed scheme for a network comprised of 16 APs, where each group of 4 APs constitutes a main cluster (denoted here by Clusters 1, 2, 3, and 4) with the same AP density per cluster. To perform soft handover, we propose forming *transition clusters* using the same APs (indicated by Clusters A, B, C, D, and E), to serve the users in multiple TSs. Similar to the single cluster case, the TSs are distributed based on the locations of the users with respect to the clusters' coverage areas. To maximize resource utilization and minimize inter-cluster interference, a TS is allocated to the main clusters to serve their users simultaneously, while the other TSs are allocated to the transition clusters, where cluster groups using the same TSs serve their users simultaneously. Note that, the use of multiple APs per cluster was also considered in RF networks for network-centric clustering in [30]. In general, our proposed solution allows applying the handover-aware scheduling with

[3]Some works define the effective SNR by dividing the calculated SNR in (2) by a factor (e.g., 10), in order to consider "more realistic" throughput, by accounting for practical limitations such as imperfect constellation shaping, signal clipping, etc. [24]. However, here we adopt the classical approach of using the SNR in (2) for calculating the achievable throughput.

[4]A division by a factor of 2 is usually considered in the literature, e.g., [25]–[27], to account for the Hermitian symmetry (HS) constraint imposed in the conventional DCO-OFDM signaling. This is not considered here. In fact, as defined in the ITU-T G.9991 standard [28], [29], it is assumed that the baseband signal is up-converted to a low intermediate frequency (IF) band with bandwidth B and central frequency of $B/2$ to avoid imposing the HS (the idea being to use the same chip-sets as for RF WiFi). This way, B in (3) denotes the bandwidth of the up-converted signal [24].

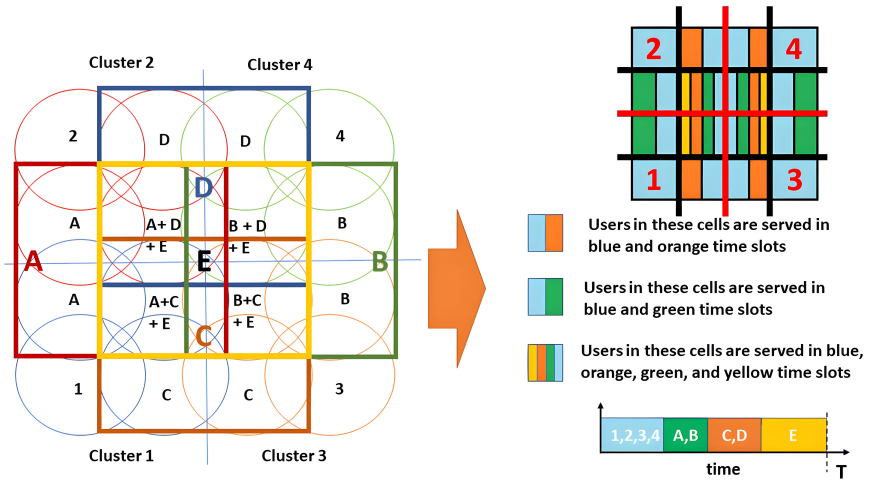

Fig. 6: Illustration of cluster formation and the corresponding resource utilization for the proposed handover-aware scheduling.

minimal reliance on the room architecture by: dividing the communication environment into several sections (with symmetry in APs locations and numbers as far as possible) and by considering the AP(s) in each section as a cluster.

In contrast to the single cluster case, due to more intersections between the clusters' coverage areas, and the control of the transmission of each AP in the cluster, users can be served using more than one TS (i.e., within TSs of the main and the transitional clusters), as shown in the right side of Fig. 6. For example, users in the upper right corner of Cluster 1 are in the coverage areas of Clusters A, C, and E, and may also be within the coverage areas of Clusters B, and D.

To simplify the illustration of the possible associated TSs for each AP's users, the right side of Fig. 6 presents TS associations for each AP coverage area, assuming that the blue TS is used by the main Clusters, the green TS is used by Clusters A and B, the orange TS is used by Clusters C and D, and lastly, the yellow TS is used by the central Cluster E. However, it should be noted that due to the large intersection areas between the transition clusters, careful management of the user association is needed: To avoid inter-cluster interference, users which are in the coverage area of two transitional clusters and use the same TS, are not served by any of them. In addition, those users covered by two main clusters can only be served in either orange or green TSs. For example, see Fig. 6, a user in the intersection area between Clusters 1 and 2 could be located in the coverage areas of Clusters C and D, which simultaneously use the orange TS, thus resulting in inter-cluster interference in the case the user is served in the orange TS. Similarly, the users covered by more than two main clusters can only be served in the yellow TS, since serving them in either blue, green, or orange TSs would result in inter-cluster interference.

B. Scheduling-Based Handover with Clustering

Consider a user moving from an initial host cluster (C_H) towards a target cluster (C_T), passing by a transition cluster (C_{TR}). For the case of conventional (non-coordinated) handover, similar to single cluster case, handover is carried out to C_T after the power from C_T (denoted by P_{CT}) exceeds the power from C_H (denoted by P_{CH}) by a HOM, i.e., "$P_{CT} \geq P_{CH}$ + HOM, over the interval TTT". This way, the user is disconnected from C_H, and handover is initiated to C_T; the user starts receiving data from C_T after link interruption of duration handover delay. On the other hand, by the proposed handover-aware scheduling, soft handover is achieved by handling the user in C_{TR}, before arriving at C_T, while being served by the corresponding TSs. As the user moves towards C_T, it passes the intersection area between C_H and C_T, where it is served only by C_{TR} to avoid inter-cluster interference.

We have summarized in Algorithm 2 the pseudo-code of the proposed handover-aware scheduling for case of a multiple cluster network. Here, P_{CTR} denotes the power from C_{TR}.

C. Comparison with the Conventional Approach

To further clarify the proposed scheduling approach, we have shown in Fig. 7 three different handover-related scenarios, for which we explain the operation of the conventional and coordinated schemes in the following. Here, as considered in the previous subsection, the user initially moves from C_H towards C_T, passing by C_{TR}, indicated in blue and red cells and green box, respectively.

- Scenario (i): The user moves totally outside C_H and arrives in C_T.
  – For the case of non-coordinated scheme, handover is initiated to C_T after satisfying the handover condition "$P_{CT} \geq P_{CH}$ + HOM over TTT", where during handover delay the user experiences link interruption, after which the user starts to receive data from C_T.
  – For the case of coordinated scheme, handover is initiated to handle the user by C_T, where during handover delay the user is served only by C_{TR}, after which the user is served in the TSs of C_T and C_{TR}. Note that the short dwell time situation occurs here with a lower probability, compared to the single cluster case, because of the larger coverage areas per cluster. It can still occur in case of user moving at cluster borders with high speed (e.g., in

Fig. 6, in case of user moving from Cluster 1 to Cluster 4, resulting in short cell dwell time within Cluster 3).

- Scenario (ii): The user moves back to C_H (ping-pong effect), remaining at the intersection of C_H and C_T.
  – For the non-coordinated case, the user will remain connected to C_T until satisfying the handover condition "$P_{CH} \geq P_{CT}$ + HOM over TTT", following which the handover is initiated to C_H and the user starts receiving data from C_H after handover delay link interruption.
  – For the case of coordinated scheme, the user is served only by C_{TR} as long as it remains at the intersection area between C_H and C_T, while experiencing no link interruption. After moving out of the intersection area, it will continue receiving data only from C_{TR}, where after handover delay it will be served by both C_H and C_{TR}.
- Scenario (iii): The user moves towards C_H (ping-pong effect) while being totally out of the coverage area of C_T before initiating handover to C_H.
  –For the non-coordinated case, the user will experience more severe link interruption than in Scenario (ii), as it would have to wait for satisfying the handover power and time conditions, in addition to handover delay, before starting to receive data from C_H.
  – For the coordinated case, user starts handover to C_H, while being served by C_{TR} during handover delay. Then, it is served by both C_H and C_{TR} in their respective TSs.

Algorithm 2 Handover-Aware Scheduling for Multiple Cluster Case

Input: P_{CH}, P_{CTR}, P_{CT}, P_C
Output: handover decision, TSs duration

```
if P_CTR > P_C then
    find clusters associated with user location
    find TSs associated with user location
    do handover to C_TR
    calculate new TSs duration
    move user data to corresponding TSs
    start D_T timer
    while D_T < handover delay do
        receive data from C_H
        increment D_T timer
    receive data from C_H and C_TR
    reset D_T timer
    if P_CT > P_C & P_CH > P_C then
        find clusters associated with user location
        find TSs associated with user location
        calculate new TSs duration
        move user data to corresponding TSs
        receive data from C_TR
    if P_CT > P_C & P_CH ≤ P_C then
        find clusters associated with user location
        find TSs associated with user location
        do handover to C_T
        calculate new TSs duration
        move user data to corresponding TSs
        start D_T timer
        while D_T < handover delay do
            receive data from C_TR
            increment D_T timer
        receive data from C_T and C_TR
        reset D_T timer
```

Overall, for the three considered scenarios, the proposed scheduling scheme offers seamless connectivity and improved link availability, compared with the conventional scheme, benefiting from the deployment of multiple intersecting clusters that offer transmission in multiple TSs.

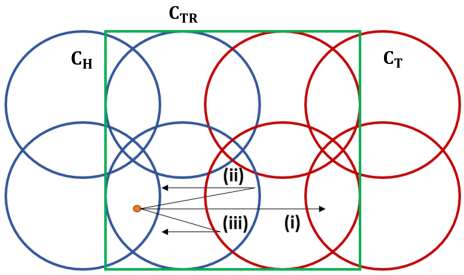

Fig. 7: Examples of handover scenarios for a user (shown in orange spot) in a multiple cluster VLC network. The blue and red cells and the green box refer to C_H, C_T, and C_{TR}, respectively.

D. Network Throughput

To investigate the network throughput, let K denote the total number of clusters. For Rx_j served by the k^{th} cluster, which is allocated the TS d_k over T, the SNR is calculated as:

$$\mathrm{SNR}_{\mathrm{Rx}_{jk}} = \frac{\sum_{i=1}^{N_t} h_{ij}^2 P_e}{\sigma_n^2}, \tag{4}$$

where $h_{ij} = 0$ if AP_i is not located in the k^{th} cluster. The achievable throughput for Rx_j is then given by:

$$R_{\mathrm{Rx}_j} = \sum_{k=1}^{K} \frac{d_k}{T} B \log_2\left(1 + \mathrm{SNR}_{\mathrm{Rx}_{jk}}\right) \quad \text{(bps)}, \tag{5}$$

where $\mathrm{SNR}_{\mathrm{Rx}_{jk}} = 0$ if Rx_j is not handled by the k^{th} cluster.

V. Time Scheduling Strategies

For the proposed the soft handover solutions, an important issue is to define the strategies for determining the TS duration, that we present in the following.

A. Single Cluster Case

We propose three time scheduling strategies as follows.

- Scheduling-S1: Here, the TS fraction with respect to signal transmission period is fixed to the associated average number of users that are served in the TS, divided by the sum of the average numbers of users in all TSs. For the i^{th} time slot fraction, this results in:

$$t_i = \frac{(N_i/N_{c,i})}{\sum_{q=1}^{Q}(N_q/N_{c,q})}, \tag{6}$$

  where N_i, $N_{c,i}$, and Q denote the number of users handled in t_i, the number of cells that use t_i for transmission, and the total number of time slots, respectively.
- Scheduling-S2: Here, the TS fraction is fixed to the maximum number of users handled in a given cell. Then:

$$t_i = \frac{(N_{i,\max})}{\sum_{q=1}^{Q}(N_{q,\max})}, \tag{7}$$

where $N_{i,\max}$ is the maximum number of users handled in a cell that uses t_i in handling users' data.

- Scheduling-S3: Here, the TS fraction is set to the sum of users handled in the TS divided by the total number of users in the network N_r. This results in:

$$t_i = \frac{N_i}{N_r}. \tag{8}$$

B. Multiple Cluster Case

We again consider three scheduling strategies as follows.

- Scheduling-S4: Here, the TS fraction for each cluster is fixed to the average number of users per cluster in the TS, divided by the sum of the average numbers of users per cluster in all the TSs. Subsequently, the cluster time slot i fraction, tc_i, is given as:

$$tc_i = \frac{(Nc_i/Nc_{c,i})}{\sum_{k=1}^{K}(Nc_k/Nc_{c,k})}, \tag{9}$$

where Nc_i, $Nc_{c,i}$, and K are the number of users served in tc_i, the number of clusters that use tc_i for handling users, and the total number of cluster time slots, respectively.

- Scheduling-S5: Here, the TS fraction is fixed with respect to the maximum number of users per cluster. Then,

$$tc_i = \frac{(Nc_{i,\max})}{\sum_{k=1}^{K}(Nc_{k,\max})}, \tag{10}$$

where $Nc_{i,\max}$ denotes the maximum number of users handled by a cluster that uses tc_i in handling users data.

- Scheduling-S6: Here, the TS fraction per cluster equals the sum of users handled in the cluster TS divided by N_r:

$$tc_i = \frac{Nc_i}{N_r}. \tag{11}$$

VI. Numerical Results

A. Simulation Methodology and Parameters

To compare the performance of the coordinated and non-coordinated schemes for the cases of single and multiple clusters, we consider a multi-cell communication environment, where each cell has an AP positioned at its center, emitting an optical power of 1.584 W [25]. The heights of the Rxs and APs are set to 0.85 and 2.5 m, respectively. The FOV of the Rx and the view angle of the LED-based AP are assumed to be 80° and 50°, respectively, where the latter corresponds to a cell radius of ∼2 m. The handover delay is set to 40 ms, given the network size and the typical handover latency in wireless protocols such as Wi-Fi or Bluetooth, which is in the range of 40 to 100 ms [31]. For both cases of single and multiple clusters, we consider 16 users, where to generate the Rx positions, the random waypoint (RWP) mobility model is used for generating 45,000 positions for each user, with successive positions being separated in time by 40 ms. For user mobility, two cases of low/moderate and high mobility are considered with maximum velocities of 0.5 and 5 m/s (with respect to the RWP model), which correspond to walking user and mobility in industrial scenarios [32], respectively. We consider a TTT of 160 ms, as in [11]. Furthermore, we assume at the central unit that the received power at the user devices is known without accounting for CSI estimation overhead in the downlink performance calculations.

For the sake of simulation simplicity, we assume that all Rxs are pointing upward toward the ceiling. Also, the users' positions in single- and multiple-cluster cases are limited to the intervals of $(1-6)$ m and $(1-11)$ m, respectively, to ensure that they are within the cells' coverage areas. Moreover, for these cases, 4 and 16 APs are considered, respectively (see Table II for the positions of the APs), where for the latter, each 4 APs form a cluster, as shown in Fig. 6. For both single and multiple cluster network cases, the time resources in any TS fraction are equally distributed among the users to mitigate multi-user interference. Note, to minimize the simulation complexity and to benefit from the relatively low user mobility in indoor scenarios, we consider a simulation time resolution of 40 ms, which is equal to the overhead delay of the handover. A smaller time resolution may be necessary when considering higher user mobility. The rest of simulation parameters are provided in Table III.

B. Comparison of Time Scheduling Strategies

Let us first compare the performances of the considered time scheduling strategies specified in Section V in order to determine the most appropriate one. Figures 8(a) and (b) show the comparison of the average achievable sum-rate for the proposed scheduling strategies for cases of single and multiple clusters, respectively. We note from Fig. 8(a) that the S3 scheduling approach offers the best performance for both considered mobility scenarios, followed by S2. For case of multiple clusters, from Fig. 8(b), S6 scheduling offers the best performance for both mobility scenarios followed by S5. These can be explained by the more opportunistic approach experienced using S3 and S6. In particular, fixing the duration of TSs based on the summation of the number of users in (8) favors CCUs in the single cluster case, because of the higher user density per TS, compared with the other CEU TSs (see coverage areas per TS in Fig. 3). In addition, considering the summation for the case of multiple clusters in (11) allocates larger TSs to the users served in the main clusters, due to a larger number of CCUs per cluster that use the TS (see coverage areas per TS in Fig. 6). The improved performance of S2 and S5 scheduling schemes, compared with S1 and S4, respectively, is due to the more opportunistic approach of the former schemes, by depending on the maximum number of users in (7) and (10) using the TS, instead of its average.

To better investigate the performance of the proposed scheduling strategies, we have shown in Fig. 9 a comparison between the cumulative distribution functions (CDFs) of the users' achievable throughput for the more demanding case of 5 m/s maximum user speed. We notice improved performance for S3 and S6 scheduling, compared with the other schemes for both single and multiple cluster cases, thanks to their more opportunistic approach. Meanwhile, we notice that S2 and S5 scheduling ensure the best performances in terms of

TABLE II: Locations of APs in the considered single and multiple cluster scenarios

Single cluster	APs (x, y, z) coordinates in meters
	(2.25, 2.25, 2.5), (2.25, 4.75, 2.5), (4.75, 2.25, 2.5), (4.75, 4.75, 2.5)
Multiple clusters	
First main cluster	(2.25, 2.25, 2.5), (2.25, 4.75, 2.5), (4.75, 2.25, 2.5), (4.75, 4.75, 2.5)
Second main cluster	(2.25, 7.25, 2.5), (2.25, 9.75, 2.5), (4.75, 7.25, 2.5), (4.75, 9.75, 2.5)
Third main cluster	(7.25, 2.25, 2.5), (7.25, 4.75, 2.5), (9.75, 2.25, 2.5), (9.75, 4.75, 2.5)
Fourth main cluster	(7.25, 7.25, 2.5), (7.25, 9.75, 2.5), (9.75, 7.25, 2.5), (9.75, 9.75, 2.5)

TABLE III: Simulation parameters

Parameter	Value
Room dimension (single cluster)	$(7 \times 7 \times 3)\,\mathrm{m}^3$
Room dimension (multiple clusters)	$(12 \times 12 \times 3)\,\mathrm{m}^3$
Number of users	16
LED luminaire Lambertian order m	1
Number of LED chips per luminaire	36 [33]
LED conversion efficiency $\mathcal{S}$	0.44 W/A [33]
Optical power per AP	1.584 W [25]
PD responsivity $\mathcal{R}$	0.4 A/W [34]
PD area	1 cm^2 [22]
System bandwidth B	10 MHz
Equivalent Rx noise power spectral density	10^{-21} A^2/Hz [34]
HOM	1 dB
TTT	160 ms
handover delay	40 ms

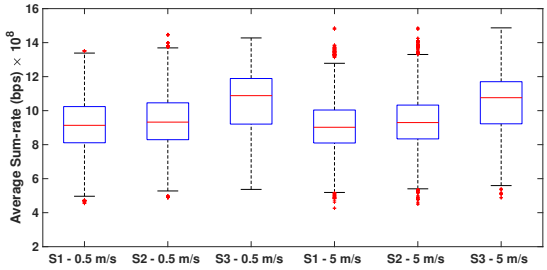

(a) Single cluster

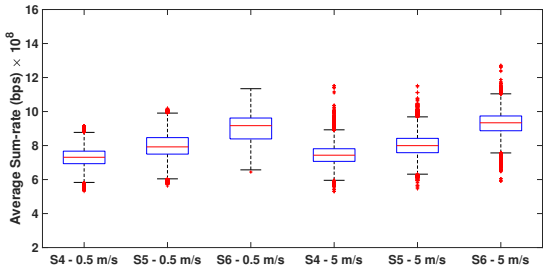

(b) Multiple clusters

Fig. 8: Average network sum-rate for the cases of single cluster with S1, S2, and S3 scheduling, and multiple clusters with S4, S5, and S6 scheduling, for maximum user velocities of 0.5 and 5 m/s.

minimum achievable user throughput (2.37×10^7 and 1×10^7, respectively), compared to S1, S3, S4, and S6 (that achieve 1.03×10^7, 2.18×10^7, 4.69×10^6, and 7.55×10^6, respectively) which reflects an improved link reliability for the users. In fact, as S3 and S6 rely on the total number of users using each time slot, they may result in allocating much larger resources to CCUs and users in main clusters, respectively, as their time slots are transmitted in parallel (see Figs. 3 and 6), which may result in low values for minimum achievable throughput for the other users. On the other hand, as S2 and S5 consider the maximum number of users per cell and cluster that utilize the time slot, respectively, and given the higher probability of having large consistency in such parameter among cells/clusters, higher values for the minimum achievable throughput are more probable. For S1 and S4, given that they rely on the average number of users per cell and cluster that use the time slot, respectively, and given that CCUs and users in main clusters are distributed among four cells/main clusters, the rest of the users may be allocated larger time resources than CCUs, while benefiting from joint transmission, thus resulting in low minimum achievable throughput for CCUs and users in the main clusters.

Based on the results of Figs. 8 and 9, S2 and S5 scheduling schemes are proposed as the most suitable as they offer a good trade-off between the network sum-rate and the minimum user throughput. In the sequel, we consider these schemes and compare their performance with non-coordinated handover.

C. Comparison of Network Throughput

To show the advantages of the proposed coordinated handover schemes, we consider different non-coordinated approaches. For the single cluster case, we adopt the conventional approach of distributing the resources (i.e., TSs) equally among the users in the network; or considering resource reuse (similar to the concept of frequency reuse in OFDMA [35]). In the latter, CCUs are served simultaneously by all APs, while CEUs in every cell are served non-simultaneously for ICI mitigation, such that different resources are allocated to CCUs and CEUs, as considered in [26]. Also, the TS duration is calculated based on the average number of users that use it. The comparison also includes the case of soft handover while relying on fractional resource reuse, as proposed in [16]. In order to adapt this latter to our case and for a general network architecture, we consider time-domain resource distribution with a reuse factor of 4 to mitigate ICI as the coverage areas of the 4 APs are largely intersecting (in [16], a reuse factor of 3 was considered assuming hexagonal cells). For the multiple cluster case, we do not consider the second and third approaches, and distribute the resources equally among the users in the network. The reason is the small intersection areas between the clusters, compared with the cluster size.

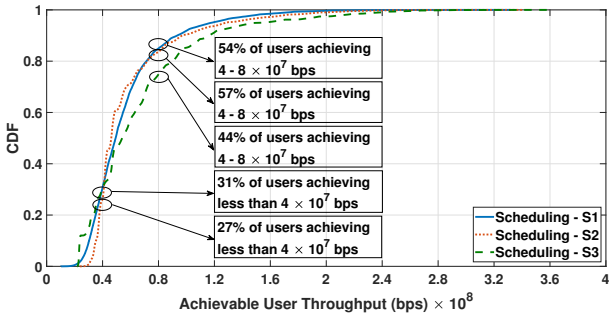

(a) Single cluster

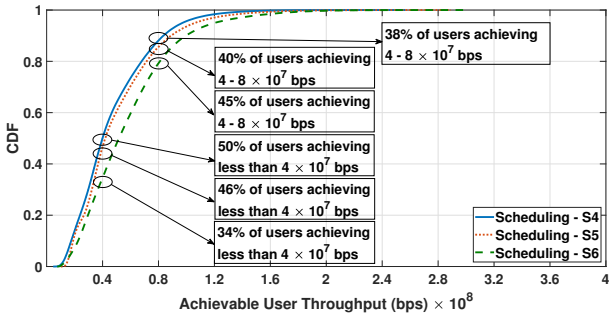

(b) Multiple clusters

Fig. 9: CDFs of the user achievable throughput for the proposed scheduling strategies in the cases of single cluster (S1, S2, and S3) and multiple clusters (S4, S5, and S6) with the maximum user velocity of 5 m/s.

Figure 10 compares the CDFs of the user achievable throughput using coordinated and non-coordinated schemes, for both single and multiple cluster scenarios. We first note that, due to equal resource allocation, non-coordinated solutions that do not consider resource reuse offer maximum fairness to the users, which is represented in the slope of the CDF. On the other hand, for the single cluster case, considering resource reuse offers a better throughput performance, due to a better utilization of the network resources. The proposed handover-aware scheduling outperforms all non-coordinated schemes, as it offers a higher user-achievable throughput, as well as a better minimum user throughput in the single cluster case, due to benefiting from joint transmission and efficient resource utilization. Note from Fig. 10(b) that, considering the fractional resource reuse for soft handover has resulted in reduced handover delay, yet at the expense of degraded performance, compared with the proposed coordinated scheme as well as the non-coordinated scheme with resource reuse. This inefficiency of resource utilization is due to the independence of resource allocation on the number of users and the large reuse factor of 4 used here.

Note, the effect of handover delay in the case of maximum speed of 0.5 m/s is small compared with the case of 5 m/s, due to the lower handover rate. In addition, the effect of link interruption during handover delay is more noticeable for the single cluster case, which could be attributed to a higher handover rate, due to a smaller coverage area per transmission.

To investigate the performance of the proposed schemes

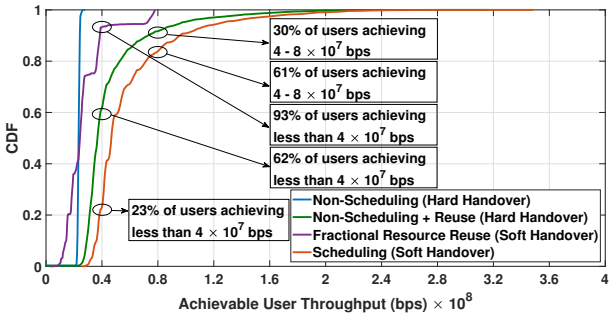

(a) Single cluster - 0.5 m/s

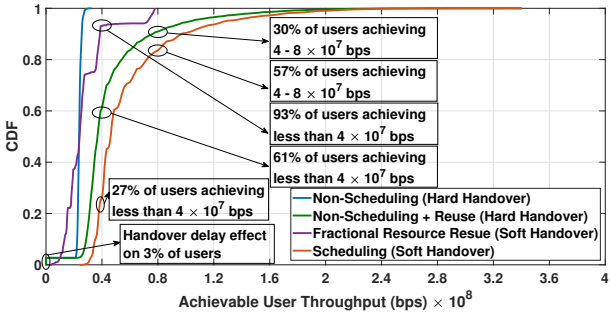

(b) Single cluster - 5 m/s

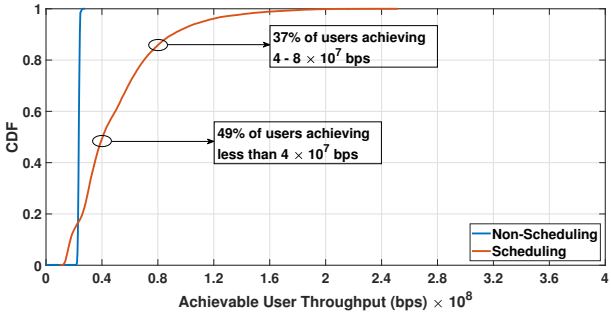

(c) Multiple clusters - 0.5 m/s

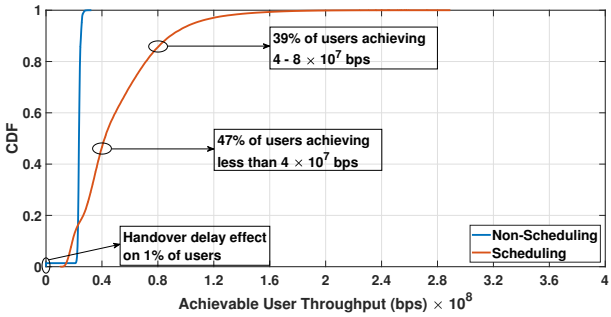

(d) Multiple clusters - 5 m/s

Fig. 10: CDFs of the user achievable throughput using non-coordinated handover and the proposed scheduling schemes in the cases of single and multiple clusters for maximum user velocities of 0.5 and 5 m/s.

under more practical conditions, Figs. 11 (a) and (b) provide the achievable throughput while considering random Rx orientations. Here, the coordinated and non-coordinated schemes

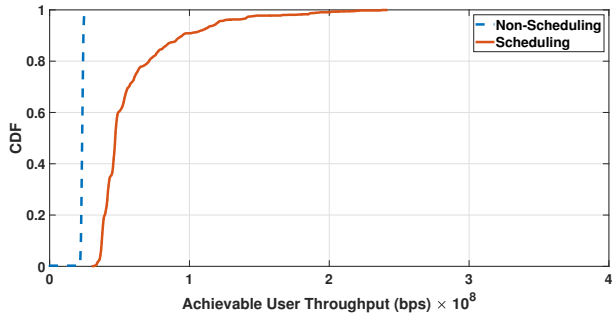

(a) Single cluster

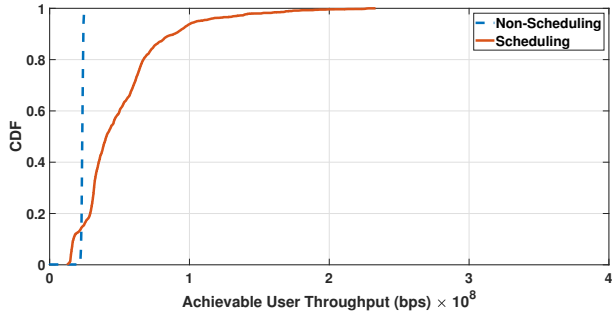

(b) Multiple clusters

Fig. 11: CDFs of the user achievable throughput while assuming random Rx orientations, using non-coordinated handover and the proposed scheduling schemes in the cases of (a) single cluster and (b) multiple clusters, for maximum user velocity of 0.5 m/s.

are contrasted for random Rx elevation and azimuth angles within the range of $(0°-30°)$ and $(0°-180°)$, respectively, over 1500 user positions generated by the RWP mobility model, for a maximum user speed of 0.5 m/s. The results show a similar performance for the scheduling and non-scheduling schemes, when compared with the results of considering Rxs pointing upwards in Figs. 10 (a) and (c), which highlights the superiority of the proposed schemes.

Overall, the results testify the robustness of the proposed soft handover schemes in terms of link availability and achievable throughput, which reflects in improved link reliability for mobile users and higher link rates, while enabling soft handover on wide range of use cases.

VII. Conclusions and Future Work

We proposed time scheduling-based soft handover solutions for small- and large-scale VLC networks, by benefiting from efficient resource utilization and joint transmission in the cell-edge areas. We compared the performances of different time slot sizing strategies, and showed that allocating the time slot duration based on the maximum number of associated users offers a good trade-off between the network sum-rate and the minimum achievable throughput. Following this, we compared the performance of the proposed schemes with conventional (non-coordinated) schemes, in terms of the achievable throughput and link availability. The results have shown that for instance, for the single cluster case, the proposed handover-aware scheduling allowed up to 60% of users to have achievable throughput ranging between $(4-8\times10^7)$ bps, compared with 30% when using non-coordinated based schemes. The main advantages of the proposed schemes include addressing user mobility while ensuring higher link reliability, improved efficiency of resource utilization thus resulting in higher network throughput, and their applicability to diverse scenarios.

It is worth mentioning that, to improve the network fairness, careful consideration of the time scheduling is needed, especially for the multiple cluster case. Also, in case of applying the proposed schemes to different room shapes, when using different light sources, the central unit should have information on the light sources (APs) including their locations, illumination levels and patterns, and use them together with the minimum received power at the user device to estimate the coverage area of each cell. Indeed, the formation of the clusters is chosen mainly based on the locations and the numbers of APs. Note that, for the case of multiple clusters, due to the Rx FOV limitations, the transmitted signals from some of the APs within a cluster may not be actually received, resulting hence in decreased resource utilization efficiency.

The advantages of the proposed coordinated handover solutions are achieved at the cost of increased network complexity, because of time slot allocation and the need for accurate synchronization. Nevertheless, the increased complexity depends on factors such as the transmission period and the required quality-of-service (QoS). For instance, real-time video streaming needs higher QoS and lower latency, hence requiring a shorter T and entailing increased complexity, compared to data transmission to simple Internet of Things (IoT) devices. In general, satisfying QoS requirements can impose constrains on the choice of the transmission periods, subsequently limiting the number of users that can be handled in the network. Also, light dimming in the VLC network limits the transmit optical power (analog dimming) and/or the used time resources (digital dimming), which can limit the maximum number of users. On the other hand, although the proposed handover-aware scheduling schemes allow avoiding ICI by using joint transmission of APs, relying on non-centralized processing in the network architecture could affect the overall network performance, e.g., due to the need for high-precision synchronization between the APs.

Another important aspect is the reliance on CSI accuracy for identifying the user location with respect to the APs, which necessitates making a trade-off between increasing the frequency of carrying out CSI estimation, and decreasing the pilot overhead used for channel estimation, depending on the channel variation rate.

Future research directions include (i) consideration of user-centric and cell-free handover solutions [36]; (ii) the combined version of proposed scheduling solutions and physical-layer MA schemes such as the spatial modulation MA [37] to optimize resource utilization; (iii) modifying the proposed handover-aware scheduling with beamforming for improving the VLC network security; (iv) evaluation of the impact of errors in the uplink transmission with respect to the proposed handover-aware scheduling; and (v) experimental evaluation of the performance of the proposed solutions.

REFERENCES

[1] Z. Ghassemlooy, L. N. Alves, S. Zvànovec, and M. A. Khalighi, Eds., *Visible Light Communications: Theory and Applications*. CRC-Press, 2017.

[2] M. W. Eltokhey, M. Khalighi, and Z. Ghassemlooy, "Multiple access techniques for VLC in large space indoor scenarios: A comparative study," in *Int. Conf. Telecommun. (ConTEL)*, July 2019, pp. 1–6, Graz, Austria.

[3] S. Al-Ahmadi, O. Maraqa, M. Uysal, and S. M. Sait, "Multi-user visible light communications: State-of-the-art and future directions," *IEEE Access*, vol. 6, pp. 70 555–70 571, 2018.

[4] Y. Wang and H. Haas, "Dynamic load balancing with handover in hybrid Li-Fi and Wi-Fi networks," *J. Lightw. Technol.*, vol. 33, no. 22, pp. 4671–4682, 2015.

[5] F. Wang, Z. Wang, C. Qian, L. Dai, and Z. Yang, "Efficient vertical handover scheme for heterogeneous VLC-RF systems," *J. Opt. Commun. Netw.*, vol. 7, no. 12, pp. 1172–1180, 2015.

[6] H. Haas, L. Yin, C. Chen, S. Videv, D. Parol, E. Poves, H. Alshaer, and M. S. Islim, "Introduction to indoor networking concepts and challenges in lifi," *J. Opt. Commun. Netw.*, vol. 12, no. 2, pp. A190–A203, 2020.

[7] A. M. Vegni and T. D. C. Little, "Handover in VLC systems with cooperating mobile devices," in *2012 Int. Conf. on Comput., Netw. and Commun. (ICNC)*, Jan. 2012, pp. 126–130, Maui, HI, USA.

[8] M. D. Soltani, H. Kazemi, M. Safari, and H. Haas, "Handover modeling for indoor Li-Fi cellular networks: The effects of receiver mobility and rotation," in *2017 IEEE Wireless Commun. and Netw.Conf.(WCNC)*, March 2017, pp. 1–6, San Francisco, CA, USA.

[9] A. B. Ozyurt, I. Tinnirello, and W. O. Popoola, "Modelling of multi-tier handover in lifi networks," in *2021 IEEE Global Commun. Conf.(GLOBECOM)*, 2021, pp. 1–6, Madrid, Spain.

[10] M. Rahaim and T. D. C. Little, "SINR analysis and cell zooming with constant illumination for indoor VLC networks," in *2013 Int. Workshop Opt. Wireless Commun. (IWOW)*, Oct. 2013, pp. 20–24, Newcastle upon Tyne, UK.

[11] X. Wu and H. Haas, "Handover skipping for LiFi," *IEEE Access*, vol. 7, pp. 38 369–38 378, 2019.

[12] S. H. Younus, A. A. Al-Hameed, and A. T. Hussein, "Novel handover scheme for indoor VLC systems," *IET Communications*, vol. 15, no. 8, pp. 1053–1059, 2021.

[13] E. A. Jarchlo, E. Eso, H. Doroud, A. Zubow, F. Dressler, Z. Ghassemlooy, B. Siessegger, and G. Caire, "FDLA: A novel frequency diversity and link aggregation solution for handover in an indoor vehicular VLC network," *IEEE Trans. Netw. Service Manag.*, vol. 18, no. 3, pp. 3556–3566, 2021.

[14] E. Torres-Zapata, V. Guerra, J. Rabadan, M. Luna-Rivera, and R. Perez-Jimenez, "VLC network design for high mobility users in urban tunnels," *Sensors*, vol. 22, no. 1, 2022.

[15] M. S. Demir, F. Miramirkhani, and M. Uysal, "Handover in VLC networks with coordinated multipoint transmission," in *2017 IEEE Int. Black Sea Conf. on Commun. and Netw. (BlackSeaCom)*, June 2017, pp. 1–5, Istanbul, Turkey.

[16] E. Dinc, O. Ergul, and O. B. Akan, "Soft handover in OFDMA based visible light communication networks," in *2015 IEEE 82nd Veh. Technol. Conf. (VTC2015-Fall)*, Sep. 2015, pp. 1–5, Boston, MA, USA.

[17] H. A. F. Camporez, W. S. Costa, J. A. L. Silva, H. R. O. Rocha, and M. E. V. Segatto, "Performance evaluation of a soft handover framework applied to VLC systems," in *2021 SBMO/IEEE MTT-S Int. Microw. and Optoelectronics Conf. (IMOC)*, Sep. 2021, pp. 1–3, Fortaleza, Brazil.

[18] M. Dehghani Soltani, X. Wu, M. Safari, and H. Haas, "Bidirectional user throughput maximization based on feedback reduction in lifi networks," *IEEE Trans. Commun.*, vol. 66, no. 7, pp. 3172–3186, 2018.

[19] K. L. Bober, S. M. Mana, M. Hinrichs, S. M. Kouhini, C. Kottke, D. Schulz, R. Freund, and V. Jungnickel, "Distributed multiuser MIMO for LiFi in industrial wireless applications," *J. Lightw. Technol.*, pp. 1–1, 2021.

[20] K. Lee, H. Park, and J. R. Barry, "Indoor channel characteristics for visible light communications," *IEEE Commun. Lett.*, vol. 15, no. 2, pp. 217–219, February 2011.

[21] S. Long, M. A. Khalighi, M. Wolf, S. Bourenanne, and Z. Ghassemlooy, "Investigating channel frequency selectivity in indoor visible light communication systems," *IET Optoelectronics*, vol. 10, no. 3, pp. 80–88, May 2016.

[22] Z. Yu, R. J. Baxley, and G. T. Zhou, "Multi-user MISO broadcasting for indoor visible light communication," in *Int. Conf. Acoust., Speech, Signal Process. (ICASSP)*, May 2013, pp. 4849–4853.

[23] *LTE; Evolved Universal Terrestrial Radio Access (E-UTRA); Radio Resource Control (RCC); Protocol Specification (Release 13), document TS 36.331 v13.0.0., 3rd Generation Partnership Project (3GPP)*.

[24] S. M. Mana, V. Jungnickel, K. L. Bober, P. Hellwig, J. Hilt, D. Schulz, A. Paraskevopoulos, R. Freund, K. Hirmanova, R. Janca, P. Chvojka, and S. Zvanovec, "Distributed multiuser MIMO for LiFi: Experiments in an operating room," *J. Lightw. Technol.*, vol. 39, no. 18, pp. 5730–5743, 2021.

[25] M. W. Eltokhey, M. A. Khalighi, A. S. Ghazy, and S. Hranilovic, "Hybrid NOMA and ZF pre-coding transmission for multi-cell VLC networks," *IEEE Open J. Commun. Soc.*, vol. 1, pp. 513–526, 2020.

[26] M. W. Eltokhey, M. A. Khalighi, and Z. Ghassemlooy, "Dimming-aware interference mitigation for NOMA-based multi-cell VLC networks," *IEEE Commun. Lett.*, vol. 24, no. 11, pp. 2541–2545, 2020.

[27] X. Deng, S. Mardanikorani, G. Zhou, and J.-P. M. G. Linnartz, "DC-bias for optical OFDM in visible light communications," *IEEE Access*, vol. 7, pp. 98 319–98 330, 2019.

[28] *High-Speed Indoor Visible Light Communication Transceiver - System Architecture, Physical Layer and Data Link Layer Specification*, ITU-T G.9991. [Online]. Available: https://www.itu.int/rec/T-REC-G.9991-201903-I/en

[29] *Unified high-speed wireline-based home networking transceivers – System architecture and physical layer specification*, ITU-T G.9960. [Online]. Available: https://www.itu.int/rec/T-REC-G.9960-201507-S/en

[30] W. Zirwas, W. Mennerich, and A. Khan, "Main enablers for advanced interference mitigation," *Transactions on Emerging Telecommunications Technologies*, vol. 24, no. 1, pp. 18–31, 2013.

[31] A. Paraskevopoulos, D. Schulz, P. W. Berenguer, J. Hilt, P. Hellwig, S. Deo, M. Bohge, T. Menzel, H. Woesner, M. Schlosser, and V. Jungnickel, "Design of a secure software-defined access network for flexible industry 4.0 manufacturing - the sesam-project concept," in *2019 Global LIFI Cong. (GLC)*, 2019, pp. 1–5.

[32] C. Sauer, M. Schmidt, and M. Sliskovic, "Delay tolerant networks in industrial applications," in *24th IEEE Conf. Emerging Technol. Factory Autom. (ETFA)*, September 2019, pp. 176–183, Zaragoza, Spain.

[33] H. Ma, L. Lampe, and S. Hranilovic, "Coordinated broadcasting for multiuser indoor visible light communication systems," *IEEE Trans. Commun.*, vol. 63, no. 9, pp. 3313–3324, Sep. 2015.

[34] L. Yin, W. O. Popoola, X. Wu, and H. Haas, "Performance evaluation of non-orthogonal multiple access in visible light communication," *IEEE Trans. Commun.*, vol. 64, no. 12, pp. 5162–5175, Dec. 2016.

[35] C. Chen, S. Videv, D. Tsonev, and H. Haas, "Fractional frequency reuse in DCO-OFDM-based optical attocell networks," *J. Lightw. Technol.*, vol. 33, no. 19, pp. 3986–4000, Oct. 2015.

[36] C. D'Andrea, G. Interdonato, and S. Buzzi, "User-centric handover in mmWave cell-free massive mimo with user mobility," in *2021 29th Eur. Signal Process. Conf. (EUSIPCO)*, Aug. 2021, pp. 1–5, Dublin, Ireland.

[37] X. Wu, M. D. Renzo, and H. Haas, "A novel multiple access scheme based on spatial modulation mimo," in *2014 IEEE 19th Int. Workshop on Comput. Aided Model. and Des. of Commun. Links and Netw. (CAMAD)*, 2014, pp. 285–289, Athens, Greece.